We are IntechOpen, the world's leading publisher of Open Access books Built by scientists, for scientists

4,800
Open access books available

122,000
International authors and editors

135M
Downloads

Our authors are among the

154
Countries delivered to

TOP 1%
most cited scientists

12.2%
Contributors from top 500 universities

WEB OF SCIENCE™

Selection of our books indexed in the Book Citation Index in Web of Science™ Core Collection (BKCI)

Interested in publishing with us?
Contact book.department@intechopen.com

Numbers displayed above are based on latest data collected.
For more information visit www.intechopen.com

4

Composite Materials for Some Biotribological Systems

Jan R. Dabrowski, Piotr Deptula and Joanna Mystkowska
Bialystok Technical University
Poland

1. Introduction

Complex functions connected mainly with directed motion, power transmission, and material forming, are performed in biotribological systems. This concerns both technical biotribological systems (machines and devices) as well as human biosystems – especially joints, and teeth and parodontium. The basic function of joints is to transmit complex dynamic loadings. Within the area of teeth and parodontium – an element of a stomatognathic system – taking nutrients and preparing them for digestive processes take place. Durability of such biotribological systems is directly reflected in the functioning of the whole human organism. Lesions and mechanical injuries of joints lead to unfavourable changes which often impede normal locomotion in humans. Similarly, in tooth systems, deterioration of hard tooth tissues, most often because of attrition and caries processes, makes normal functioning of stomatognathic systems much difficult. One of more and more popular methods applied in repairing human joints is endoprosthetics, i.e. a surgical treatment consisting in replacing a diseased joint with an artificial apparatus – an endoprosthesis. In the case of defects in hard tooth tissues, the defects are either filled or the damaged tooth is replaced with an implant. Biomaterials used for these purposes, beside having a number of biofunctional features, should have very good tribological characteristics – low friction coefficients and antiwear performance.

Progress in reconstructive surgery of human joints and in conservative dentistry, in particular selecting appropriate biomaterials and constructions, depends to a large extent on getting to know these biotribological systems, which facilitates producing more reliable functional and structural models of the systems, and thus results in developing 0more correct methods of assessing their biotribological characteristics.

Fig. 1. shows a graphical representation of a general functional model of a biotribological system, in which, beside the classical external environment, the environment of an autonomous character is marked together with the feedback of parameters characteristic of the input-output function. It is a proposal of a system functional model of the "black box" type.

It has to be emphasised, however, that transferring achievements of the methodology of biotribological research on technical systems to biological systems has to be preceded by analysing the differences between these two types of systems. Beside selecting basic parameters for making such an analysis, mainly parameters concerning kinematics of motion and loading dynamics, phenomena and their effects occurring in the autonomous

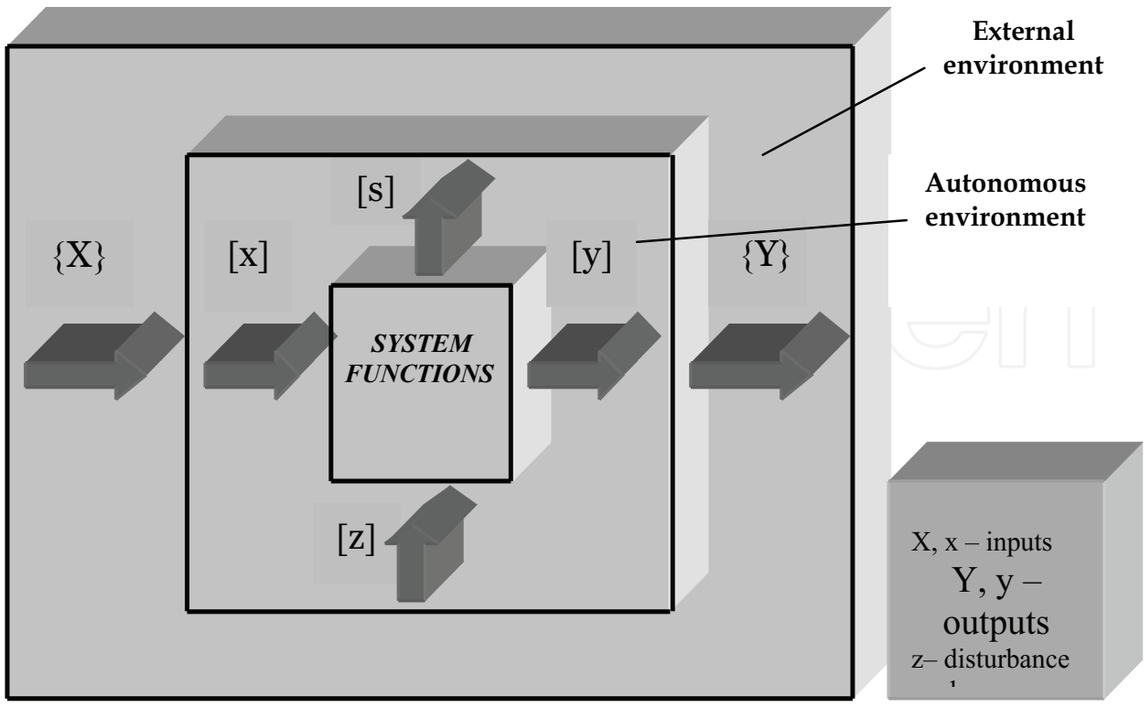

Fig. 1. General functional model of a biotribological system [5]

environment of a particular biotribological system need to be taken into consideration. An autonomous environment is characteristic of the phenomenon of homeostasis (feedback), open to incoming information and closed to energy and matter. For example, chondrocytes play a significant role as centres which regulate exchanging matter and energy within articular cartilage. The reaction of joints in degenerative arthritis, consisting in increasing the joint area and thus decreasing the pressure per unit area, is widely known. Morphological reconstruction of joint areas might also be a reaction of a healthy joint to too much mechanical loading. Reactions of morphological elements of teeth to the influence of external stimuli, characteristic of the process of homeostasis, are quite well-known: processes of reparation, or tertiary dentin forming in case of excessive tooth attrition, can be mentioned as an example.

The complexity and dissimilarity of biotribological systems in comparison to technical ones do not facilitate research experiment planning. Biotribological research and inference cannot therefore be based exclusively on theories and methodologies developed for technical biotribological systems. For that reason, special devices are constructed for biotribological research experiments, i.e. wear simulators which reflect motion kinematics and dynamics of loadings in the analysed system as closely as it is possible. Descriptions of known wear simulators of joints can be found in , and these of teeth in 2 Materials for friction pairs of artificial joints

2. Materials for hip endoprotheses

2.1 Introduction

A hip joint endoprosthesis is composed of a metal stem, fixed in the femoral bone, an acetabular cup (most often a polyethylene or ceramic one, placed in the pelvis), and a head

(metal or ceramic) frictionally cooperating with the acetabular cup. A diagram of an endoprosthesis is presented in Fig. 2. Selecting appropriate materials, based on the concept of Charnley's 'low friction arthoplasty', was a breakthrough in endoprosthetics of human joints. Applying a metallic head (austenitic steel, implant alloys of cobalt) and an acetabular cup made of high-molecular polyethylene (UHMWPE) made it possible to construct commercial endoprostheses which have been most widely used so far. However, neither patients nor doctors find the average time of using endoprostheses, which is 10-15 years, fully satisfactory. Moreover, unfavourable influence of wear products (toxic, immunogenic, mutagenic, etc.) of endoprostheses, osteolysis around implants, and finally, surgical difficulties of re-alloplastics (repeated implantation) are very important reasons for further research in the field of construction material solutions to be applied in human joint endoprostheses. Much hope is placed in this aspect in the development of composite materials for endoprosthetics. A particularly significant research task is connected with applying new titanium alloys – without toxic additions of vanadium or aluminium, and with better tribological characteristics. It has to be underlined that titanium alloys are not used in friction nodes of endoprostheses due to the high susceptibility of these alloys to tribological wear and their frictional resistance.
The subject of the authors' own research was the development of new composite materials based on implant alloys of cobalt and titanium, with special emphasis on shaping the biotribological characteristics of these materials.

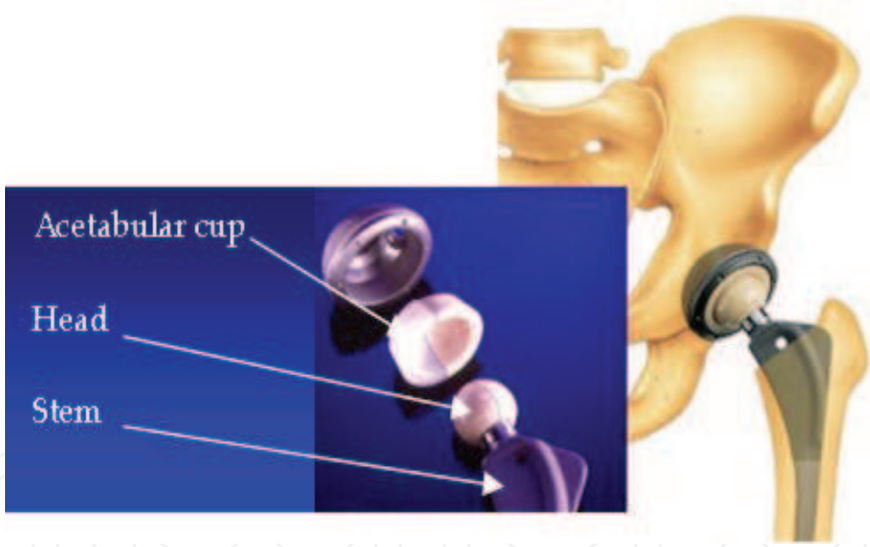

Fig. 2. Construction of a hip joint endoprosthesis

2.2 Investigated materials

The specimens were fabricated by means of the powder metallurgy method. Composite materials based on Co-Cr-Mo powders as well as titanium powders were used for the tribological tests. Co-Cr-Mo powders with 10% weight fraction of $Ca_2P_2O_7$, BN, Si_4N_4 and titanium powder with 10% and 20% volume fraction of graphite (Ti + C) as well as 10% and 20% volume fraction of titanium carbide (Ti + TiC) and 2% volume fraction of yttrium were investigated (Table 1.). The basic powders with friction modifiers were dry-mixed in a Pulverisette 6 planetary ball mill for 15 minutes. Some of the initially mixed powder was milled in a SPEX 8000D high-energy shaker mill in a protective argon atmosphere

(mechanical alloying). All the powder mixtures were cold-pressed in a matrix under the pressure of 600 MPa. The mouldings were sintered in a tube furnace in a protective atmosphere (a vacuum of 10^{-5} mbar) for 3 hours at the pipe temperature of 1230°C. The mouldings based on Cr-Cr-Mo powders were sintered for 1 hour. The specimens were cooled down naturally to the ambient temperature inside the furnace.

Material			
Co-Cr-Mo sinters		**Ti sinters**	
Symbol	*Composition*	*Symbol*	*Composition*
S0	Co-Cr-Mo alloy	**T0**	Pure titanium
S1	sinter	**T1/10**	Ti+10%C
S2	sinter+$Ca_2P_2O_7$	**T1/20**	Ti+20%C
S3	sinter+BN	**T2/10**	Ti+10%TiC
S4	sinter+ Si_3N_4	**T2/20**	Ti+20%TiC
-	-	**T3**	Ti+2%Y_2O_3

Table 1. Chemical composition of the investigated composites based on Co-Cr-Mo and titanium

2.3 Tribological tests

The microstructures of the composite materials were observed under a Hitachi S-3000N scanning electron microscope with an X-ray NSS microanalyser. Maps of the location of the elements, a line analysis of the elements appearance, and a chemical composition analysis were also made by means of scanning microscopy. An X – ray diffraction analysis for the powder samples after different times of mixing, heating in a calorimeter and consolidation were made with a Rigaku MiniFlex II, applying the CuKα (λ = 1.54178 Å) radiation. To assess the average size crystallites and the average amount of net defects, the Williamson-Hall method was used. Hardness was measured with the Brinnel method, while microhardness was measured with the Vickers method with a Neophot-21 ($\mu HV_{0,1}$) optical microscope.

The tribological tests were performed with a special tribometer using a reciprocating ring-on-disc system. Schematic diagrams of the tribometer are presented in Fig. 3. The research was conducted during the periodically variable motion with low velocity and variable values of pressure. The tribological tests were performed with tribometer using reciprocating ring-on-disc system with an angular displacement f = 0.24 and a frequency of 1 Hz. The research was conducted during the periodically variable motion with low velocity and pressure variable values. The ring was loaded along its axis, and the loading was changing within the range of 0 to 350N (the maximum contact pressure p_{max} = 2MPa). The maximum value of sliding speed was v_{pmax} = 0.018m/s.

The friction coefficients were calculated from the maximum values of the friction force to describe extreme resistances to motion. The geometry and dimensions of the tribological pair are shown in Fig. 3. The investigated sintered composites (with 10 and 20% addition of graphite, 10 and 20% addition of titanium carbide, and composites with yttrium) were used as discs, while the counterspecimen in the form of a ring was made of a bulk titanium alloy.

In the case of Co-Cr-Mo sinters, the couterspecimen was a bulk Co-Cr-Mo alloy. The tribological tests for the composites based on Co-Cr-Mo were carried out in a distillation water environment and a CMC environment. The quantitative research was performed by two methods – on the grounds of the roughness measurements and by volume measurements for the sinters based on Co-Cr-Mo powders and by weight measurements for the composites based on titanium. In this paper, a T8000-R60-400 Hommeltester profilograph with the possibility of friction simulation on investigated surfaces was used.

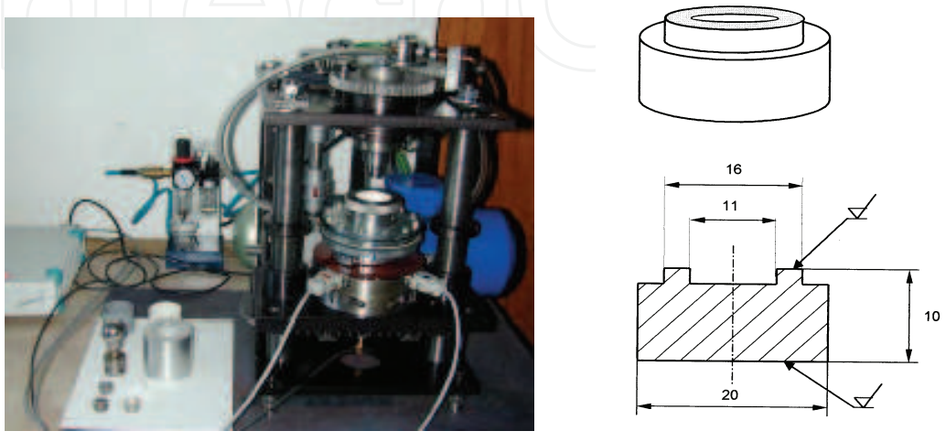

Fig. 3. The tribometer and the geometry of the tribological pair

The device may be used for testing head/acetabular cup or ring/disc kinematic systems. A kinematic pair is placed in a specially constructed container providing for continuous lubrication (forced circulation of the lubricating fluid). The loading was applied as a sinusoidal cycle, with the head (ring) moving in a reversible way, and the specified initial interspace between the friction faces. The possibility to pre-set the size of the initial interspace between the friction faces corresponds to physiological conditions influencing the functioning of the human hip joint. It is also possible to select the point of application of loadings normal to motion coordinates and to regulate the period and amplitude of loadings. The presence of the interspace between the friction faces and its size are some of the most important parameters which influence creating appropriate conditions of lubricating artificial joints.

The prepared samples of porous implantation materials were compressed with an INSTRON 8502 strength testing machine and further the compression curves were analysed.

2.4 Results and discussion

For composites based on Co-Cr-Mo powder, the *Ra* initial surface roughness of the composite samples based on Co-Cr-Mo powder was determined to be of the order of ~ 0.06...0.11 μm. The loading was applied in the first part of the friction cycle (the first half of the sinusoidal loading period), reaching the maximum pressure of 10 MPa. The size of the initial interspace was determined to be of the order of 0.2...0.3mm. Changes in the rubbing speed and in the values of loadings as well as these in the friction force were recorded in a continuous way. After the test was finished, the lubricating fluid was collected, and the contents of chromium and cobalt in the fluid were determined using Atomic Absorption Spectrometry (AAS, Z5000 Hitachi). The friction faces were observed with the use of a scanning microscope (SEM, Hitachi 3000N).

The observed changes in the roughness of these surfaces were assessed using a Talysurf 10 (Taylor-Hobson) profilometer. The volume wear was assessed with a planimeter from the profilograms for the friction surfaces of the plates in the radial direction. R = 7mm was adopted as the (r) mean friction radius. Biotribological characteristics of the following groups of materials obtained on the basis of powder III were determined.

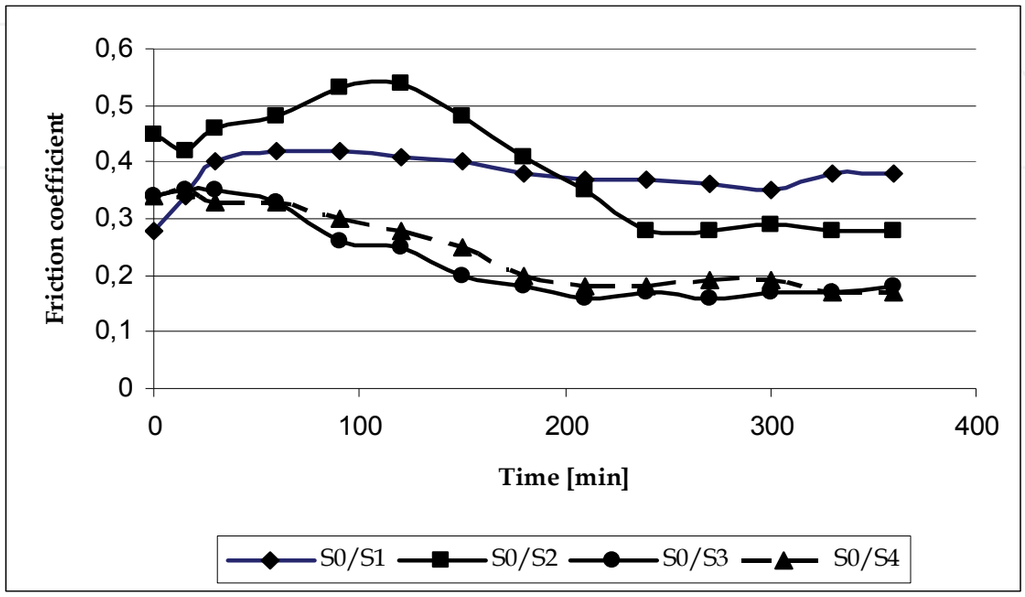

Fig. 4. Changes in friction coefficients of the tested materials in the time function

As it can be seen from Fig. 4., after the running-in period, stabilisation of the friction coefficient takes place in the tested materials. The presented data indicate that the friction coefficients for the composites with the addition of silicon nitride and boron nitride were twice as small as those for the moulding/pure sinter pair. However, in terms of tribological efficiency, the results for calcium pyrophosphate were distinctly worse in comparison to these of the tested friction modifiers.

The tribological wear of the materials under research was assessed on the basis of the cobalt and chromium contents in the lubricating fluid as well as on the basis of profilograms for the friction surfaces of the moulding plates (the volume of wear products). The results of these tests are listed in Table 2.

Friction pairs	Content of elements, [ppm]		Volume wear, x 10^{-3} mm^3
	cobalt	*chromium*	
S0 / S1 (pure sinter)	7.16	2.72	1.29
S0 / S2 ($Ca_2P_2O_7$)	9.51	10.20	2.05
S0 / S3 (BN)	3.68	2.72	1.07
S0 / S4 (Si_3N_4)	1.95	1.99	0.65
lubricant	6.45 x 10^{-3}	5.62 x 10^{-3}	-

Table 2. Results of wear measurements

The data presented in Table 2. are indicative of a favourable influence of boron nitride and silicon nitride on decreasing wear in comparison to the data for pure sinter. The composites containing silicon nitride have the best anti-friction and anti-wear characteristics, whereas the addition of calcium pyrophosphate – contrary to the expectations – unfavourably influenced both the motion resistance and the wear of the tested materials.

Tribological characteristics of the obtained composite materials depend to a large extent on the anti-friction and anti-wear efficiency of the introduced additions, the material cohesion, and the surface morphology. The performed microscopic observations show that composites with the addition of silicon nitride have the most favourable structure of top layers (Fig. 5a). An analysis of photographs of the surface of this composite indicates that the top layer material is characterised by good cohesion. The surface is smoothed, with small irregular pores and clearly visible light areas containing silicon nitride. Photographs of friction surfaces of composites with calcium pyrophosphate and boron nitride are quite dissimilar. Observations of the surfaces of sinters with the addition of calcium pyrophosphate (Fig. 5b) show that this addition unfavourably influences the processes of sintering cobalt powder particles, and thus the cohesion of the obtained composites. In photographs of surfaces of such composites, the presence of additions surrounded by non-sintered particles of cobalt alloy powder is clearly visible. This decreases the material cohesion and thus increases the possibility of metallic particles to be crumbled out from the surface during friction. A loss of calcium pyrophosphate from surface pores in the friction process is also observed.

It is most probably caused by a low internal cohesion of this phase and its elution by the lubricating fluid. Similar surface structures were observed in boron nitride composites, with characteristic numerous discontinuities occurring at the phase border between the metal particles and the additive, which is indicative of a low interphase cohesion of these materials.

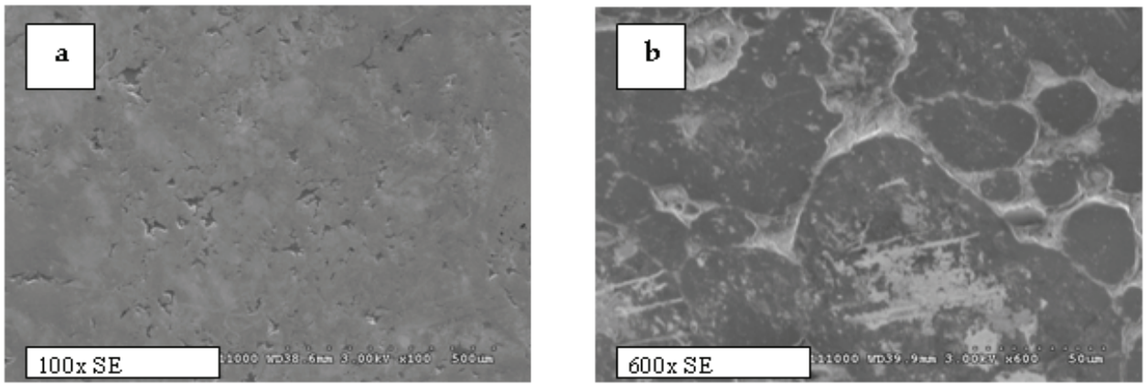

Fig. 5. Microstructure of friction trails: a) S4 (Si_3N_4), b) S2 ($Ca_2P_2O_7$)

The results of the performed tests reveal that the composites containing silicon nitride have the most favourable tribological characteristics and therefore silicon nitride seems to be an effective anti-friction and anti-wear additive to porous materials based on a Co-Cr-Mo alloy. The idea of using such composites to construct friction nodes of endoprostheses might be supported by a wide application of materials of this type in tribotechnics and by promising literature data concerning applying silicon nitride composites or even its sinters in friction nodes of endoprostheses.

For the titanium composites, the first experimental part included structural tests on the alloys manufactured with traditional powder metallurgy methods without alloying powder mixtures. The green specimens of composites with graphite, titanium carbide, and the addition of Y_2O_3 before sintering were characterized by good compactibility. The relative density of the received Ti+C molder was about 83%, which could be explained by a good lubricating effect of graphite during the compaction process. The material with the addition of graphite of 93% showed the largest compactibility after sintering. This indicates the possibility of a thermally activated reaction taking place between the components during sintering. The relative density of other composites was minor in each case (Fig. 7).

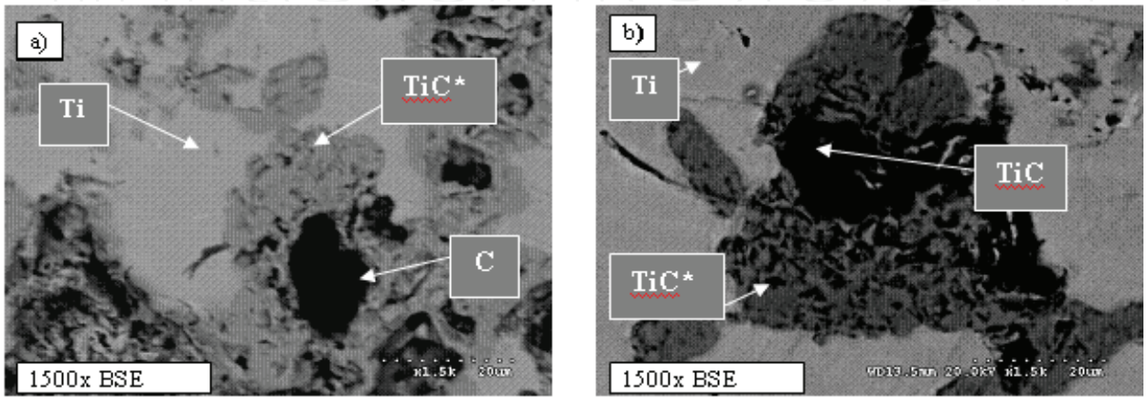

Fig. 6. Microstructures of composites: Ti + graphite sintered in 1230◦C, b) Ti + titanium carbide sintered in 1230◦C

The microstructures of the composite materials with titanium modifiers confirmed this fact. As a result of diffusion, a new phase titanium carbide appeared on the border between the titanium grains and graphite. The obtained materials were composed of a soft titanium warp, graphite or titanium carbide residuals, and a secondary hard phase of carbides – TiC* (Fig. 6). It may be supposed that such a material would have very good tribological properties.

Fig. 6. shows that interactions between the metallic basis and modifier (graphite and titanium carbide) during sintering were observed.

At the second stage, samples of sinters after mechanical alloying were investigated. The titanium and graphite powder mixtures underwent the mechanical alloying processes. The mechanical alloying favourably influenced the solubility of carbon in titanium and the creation of a large amount of secondary carbides. The obtained powders underwent consolidation through the processes of pressing and sintering. In the SEM image of the samples of the obtained sinters, sintered titanium powder grains with dissolved carbon as well as precipitations of titanium carbides on the grain borders are clearly visible. These results were confirmed by rentgenostructural tests. Composites after mechanical alloying were characterised by a lesser compaction. This results from the fact that friction between nanoparticles was much bigger during compaction, which causes less compaction in the process of pressing. As a result of the mechanical alloying, a significant fragmentation of the powder structure occurred. The X – ray crystallography and microscopy (TEM) studies show that the powder grain size was 20 – 120nm.

A good correlation was found between the structural analysis and the hardness of the investigated composites. The results of macrohardness measured with the Brinnel method,

as well as the average microhardness of the material, showed a significant influence of the sintering temperature on the composite properties.

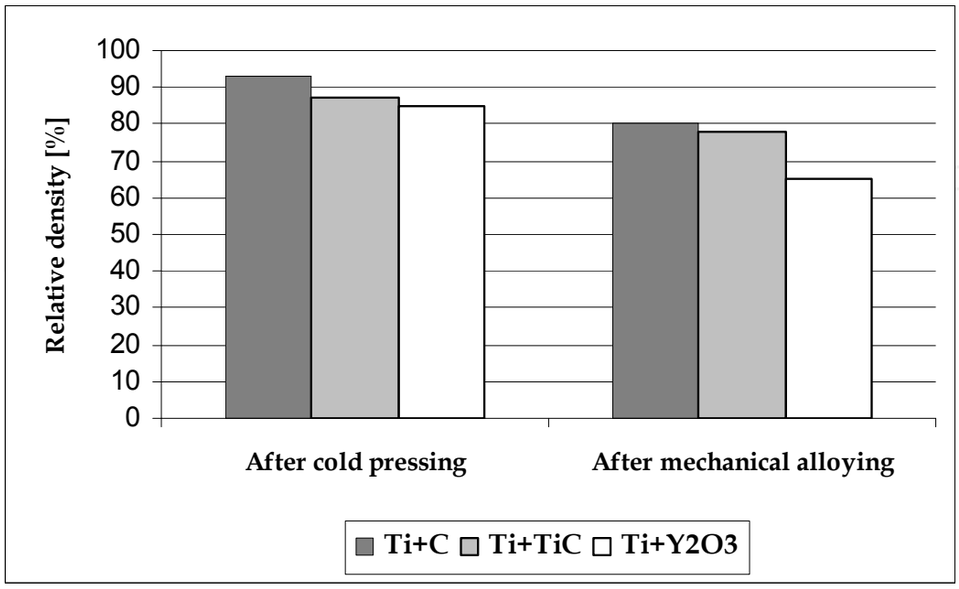

Fig. 7. Results of relative density measurements for investigated composites

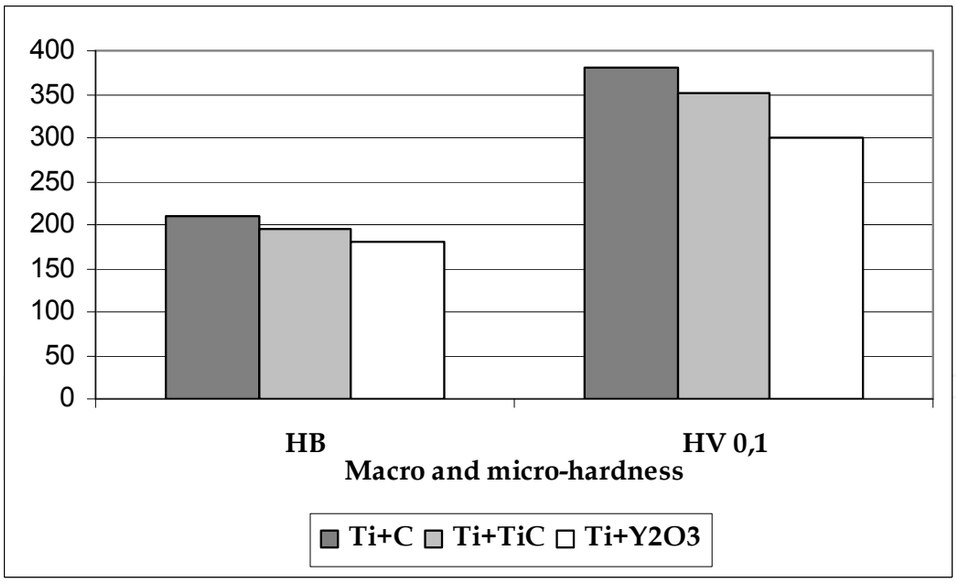

Fig. 8. Results of macro- and microhardness measurements of specimens

The macrohardness of the titanium-graphite composites sintered under the temperature of 950^{o}C was approximately 90HB, whereas the hardness of pure bulk titanium amounted to 83,4HB. The macrohardness of the titanium-titanium carbide composites sintered under the temperature of 950^{o}C was approximatly 85HB. The hardness value of the composites with graphite sintered under 1230^{o}C was similar to the value for high-carbon normalized steel (Fig. 8).

The macro-hardness micro-hardness test in the neighbourhood of graphite confirms that it indeed is a hard phase. The obtained material was composed of a soft titanium warp, graphite residuals and a secondary hard phase of carbides (Fig. 6). It may be supposed that such a material would have very good tribological properties.
The results of the microhardness tests on the obtained sinters, listed in Fig. 9., and Table 3., indicate that mechanical alloying favourably influenced the increase in the microhardness of the produced materials. The composite materials with the addition of graphite were characterised by the greatest hardness. It has to be emphasised that the microhardness of such composites, after the mechanical alloying process, increased to very high values of the range of 900 HV0.1.

Microhardness HV 0.1	**Ti+C**	**Ti+TiC**	**Ti+Y_2O_3**
Powder metallurgy	380	352	300
Mechanical alloying	820	-	450

Table 3. Results of microhardness measurements of specimens after P.M. and mechanical alloying

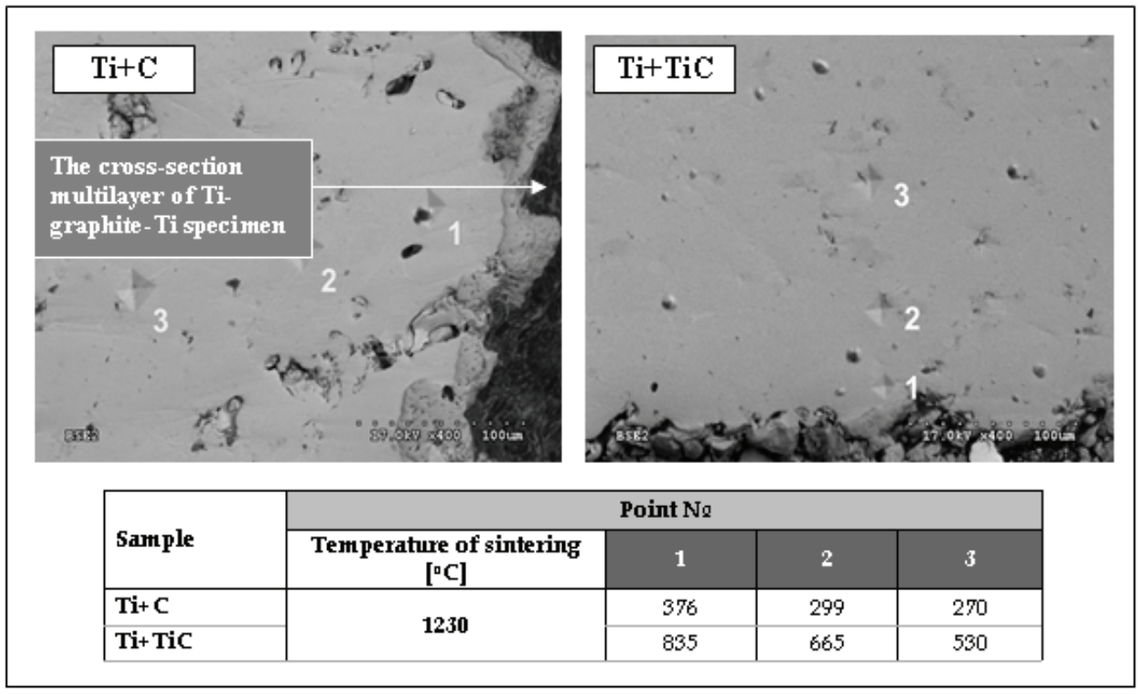

Sample	Point №			
	Temperature of sintering [°C]	1	2	3
Ti+C	1230	376	299	270
Ti+TiC		835	665	530

Fig. 9. Influence of carbon diffusion on microhardness of titanium samples

A comparison of the friction coefficient values for the investigated materials is shown in Fig. 10. The analysis of the obtained results confirmed a good influence of graphite on tribological properties of the sinters.
The friction coefficients for the composites with graphite reduced over twice compared with friction of pure titanium samples. The values of the motion resistance are also lower for the composites with titanium carbide, although to a lesser degree than in the case of the composites with graphite. In two cases, the influence of modifiers is clearly visible – an

increased volume of the fillers caused a decrease of the friction coefficients. The quantitative research was performed on the basis of the roughness measurements and by weight measurements.

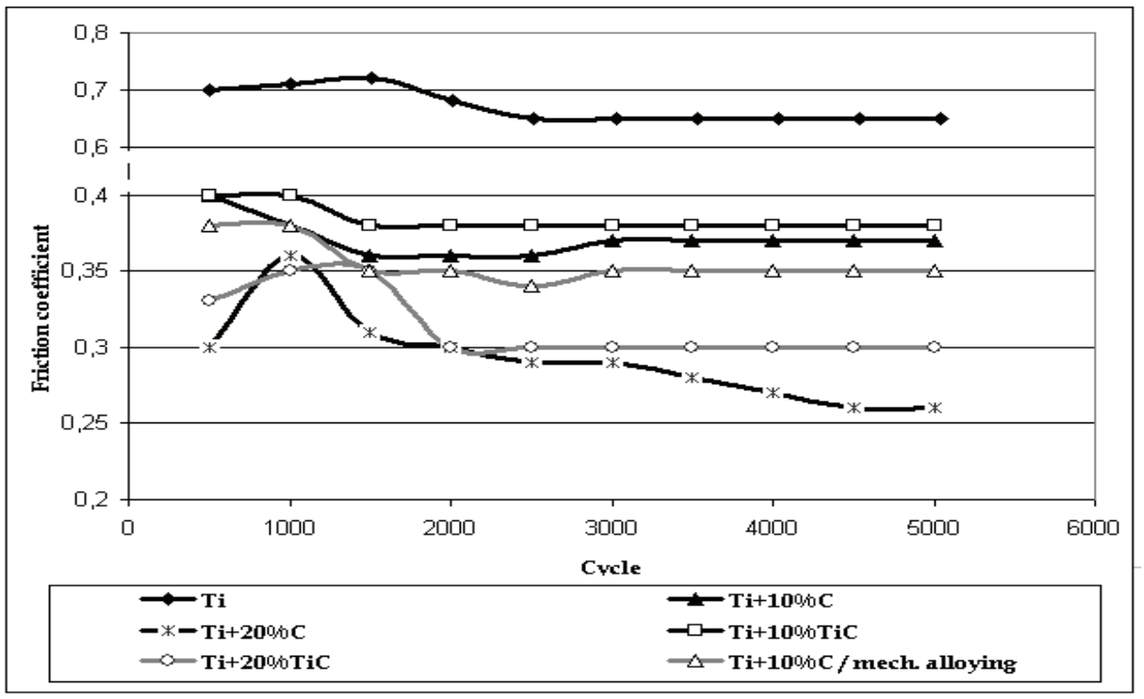

Fig. 10. Influence of graphite and titanium carbide on composite tribological properties of investigated composites

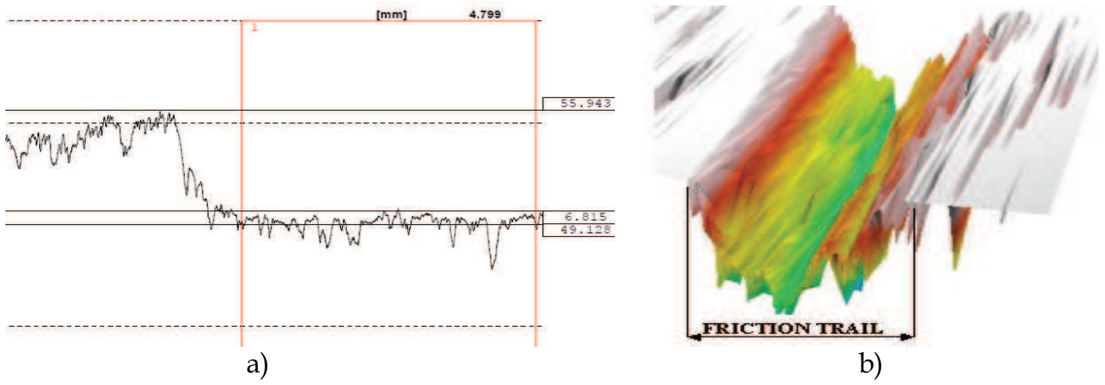

a) b)

Fig. 11. Friction trail of Ti+20%TiC composite: a) roughness measurement, b) wear simulation

Examples of profilograms and wear simulation of the friction surface of Ti+20%TiC are presented in Fig. 11., whereas Table 4. shows the wear of the investigated materials. Significant decreases in the wear for the samples with graphite, and increases in the wear for the samples with titanium graphite in comparison to pure titanium sinters can be observed. For the composite with 20% volume fraction of graphite, the friction coefficient after 1h of

tribological testing was at the level of 0.27, which confirmed good lubrication conditions during friction. The wear for this composite, measured after the tribological test was of the range of about 9.8 g ·10^{-3} (Table 4). This material had the best tribological properties.

Sample	Wear loss	
	Linear wear [μm]	*Weight wear *10^{-3} [g]*
Pure titanium	30.4	21.5
Ti + 10% C	16.6	11.5
Ti + 20% C	9.8	7.2
Ti + 10% TiC	33.9	23.7
Ti + 20% TiC	49.1	35.8

Table 4. Results of wear tests

A significant influence of the volume of the fillers on the wear volume is visible. In the case of the Ti+C composites, the wear decreases, while in the case of the Ti+TiC composites it increases. An advantageous influence of the graphite addition on decreasing the motion resistance and wear of the obtained composites should be underlined, which will have a significant meaning in technical aspects.

The less advantageous tribological characteristics of Ti+TiC composites results from lower cohesion of this type of materials and demolition of hard TiC particles, which is connected with this. This demolition might cause intensifying of secondary wear processes, which was confirmed by the observation of friction surfaces of the samples after friction.

The abrasive and fatigue wear is dominating with the visible deformation areas and spalling of the surface layer in the friction surfaces. In the case of the Ti+TiC sample, small particles of filler loosely connected with the surface, can be seen. This might cause intensification of wear processes.

The obtained results are indicative of a better compatibility and more advantageous mechanical properties of the Ti+C composites. The presence of reactive phases between the titanium and graphite particles has an advantageous influence on the cohesion and properties of this type of composites.

The performed tribological studies also indicate a favourable effect of mechanical alloying on the tribological properties of the alloy. The sinters made of the powders after mechanical alloying were characterized by a lower coefficient of friction (Fig. 10) and higher tribological wear resistance. It is an important feature of this kind of implant materials as regards capabilities of applying them in friction nodes of biomedical devices.

3. Materials for dental fillings

3.1 Introduction

Amalgams, glass-ionomers, compomers and composites are materials for dental fillings. Composites stand out against the group and are often applied on teeth mainly due to their good mechanical and aesthetic properties. Dental composites are built of both organic (i.e. a system of monomers, polymerization initiators, stabilizers, pigments, accelerators etc.) as well as inorganic components such as powder and fiber fillers. A silane coupling agent connects these two phases and plays a key role in enhancing the adhesion of the interface

between the inorganic powder and organic polymer. On the other hand, silane, due to its low reactivity, brings about a decrease in material polymerization shrinkage. The constitution of the organic matrix and fillers also plays an important part in defining final properties of materials. It is generally accepted that the properties of composites are mainly dependent on the type, size, spacing and volume fraction of the utility filler. The latest literature available on the subject points to a significant influence of fluoride sources, nanoparticles and friction additives on the structure and utilization properties of composites. It has been found that reducing the particle size to a nanoscale level has already reached a significant degree of efficiency. Among dental composites, nanosilica appears to have become the most commonly used nanopowder.

The wear of dental materials is one of the major problems concerning almost every kind of dental filling. As far as dental materials are concerned, there are a few main types of wear processes: abrasive, adhesive and fatigue. Generally, the wear of a filling material should be comparable with the wear of human enamel. The ultimate goal of advanced dental material studies is to produce a material that can be used in all circumstances as an amalgam replacement material which revealed an optimal wear resistance. The best way of developing such a material is to combine it with composite materials for dental fillings. In order to reduce the wear and coefficient frictions of the analyzed materials, the composition of the applied fillers is modified. The addition of hard corundum particles, aluminium and glass fibres have a positive effect on mechanical properties only. An evident improvement of the tribological properties of a material can be obtained by using a suitable filler, called friction modifier. In the case of inorganic fillers, the wear of the material is probably connected with the sum of damage caused to the silane coupling agent. The composites with the highest degree of coupling show the highest wear rate. Recently, ceramic whiskers were used to reinforce dental resin composites. Xu and others demonstrate that silica-fused whisker reinforcement produced dental resin composites that exhibited high resistance to wear with smooth wear surfaces. Generally, inorganic particles are well known to enhance the mechanical properties of polymers, which have been widely investigated in the past decades. Different organic fillers are also applied. For example, the PTFE is applied when a reduction of the adhesion of the investigated material to the counterpart material is needed. Different methods are available for the quantification of wear, using different loads, times of investigations and sizes of samples. The type of the used wear method has a distinct effect on receiving results. The pin-on-disc is the most frequently applied tester system. Various lubricants for in vitro wear testing are also used.

Among many desirable requirements of materials for dental fillings, fluoride release is also of a significant quality. Fluoride ions play a key role in dental and enamel remineralisation. Many cases of studies show that fluorine can also be an inhibitor of a cariogenic effect of microorganisms. It decreases the risk of caries that forms in tissues directly adjacent to the filling material. Numerous investigations are made with the aim to obtain a material which would perform those tasks and would have high mechanical, physicochemical, and tribological characteristics at the same time. The best possibility for developing such a material is combining it with composite materials for dental fillings. The quickness of fluoride release depends on many factors, e.g. the kind and volume of the used fluoride source and the environment into which it is released. Fluoride ions are introduced into dental composite materials in the form of fluoridated glass or pure compounds, such as CaF2, NaF, YbF3, YF3, SrF2. However, due to an innovative approach to this problem, there is little literature data concerning the influence of dynamical loading on fluoride release

kinetics. The fluoride release may change the material structure. Therefore, the tribological, mechanical, and physicochemical properties as well as analyses of material surfaces are described in literature.

The investigations of mechanical, tribological, and physicochemical properties of some originally made composite materials for dental fillings were performed at the Department of Materials and Biomedical Engineering (Faculty of Mechanical Engineering, Bialystok University of Technology, Poland. The aim of these studies was to compare the properties of composite materials for dental fillings consisting of organic fillers of polyethylene (PE) and polytetrafluoroethylene (PTFE) with those obtained with inorganic friction modifiers of silicon nitride (Si3N4) and boron nitride (BN). In the next stage, the influence of the used loading sample on fluoride release, the surface roughness and the material structure was examined.

3.2 Tribological characteristics

At this stage of the tests, five ceramic-polymer microfilled composites containing friction modifiers were tribologically tested. The sample without a friction modifier was a standard one. Each composite consisted of a polymer matrix (40 vol. %) in which the mixture of the following organic resins was used: Bis-GMA resin {2,2-bis[p-(2'- hydroxy-3'-methacryloxypropoxy)-phenyl] propane}, TEGDMA {tri(ethylene glycol) dimethacrylate}, DEA-EMA {2-(diethylamino) ethyl methacrylate}, BHT, CQ {D,L-Camphorquinone} and a photoinitatior. All the components were provided by the Sigma-Aldrich Company. The remaining part of the composite (60 vol. %) was a mixture of inorganic powders: fluorine source and friction modifiers. The fluoridated glass (J-20 symbol) consists of: SiO_2- P_2O_5-Al_2O_3-BaO-SrO-Na_2O-F^-. The glass was worked out and prepared at the Institute of Glass, Ceramics, Refractory and Construction Materials (Warsaw, POLAND).

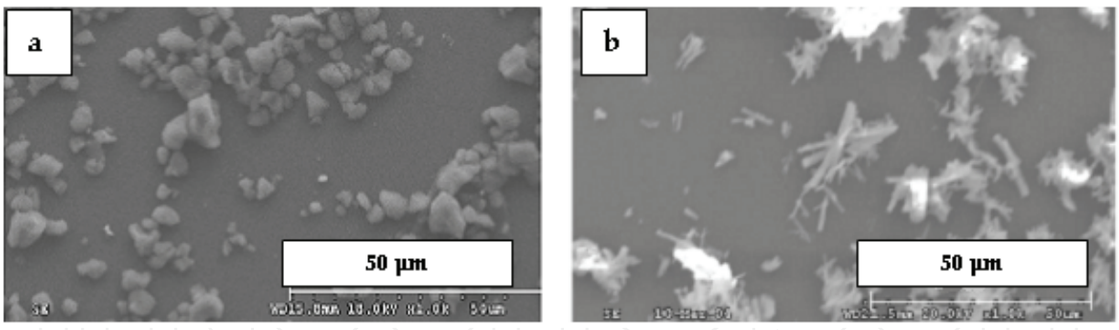

Fig. 12. SEM pictures of particle structure of used fillers: (a) PE, (b) Si3N4

The friction modifiers including Si3N4, BN, PE, and PTFE were also delivered from the Sigma-Aldrich Company. Each of the listed powder fillers is distinguished by various forms and sizes of the fillers. PE, PTFE and BN have irregular grains of different particle dimensions. Silicon nitride whiskers were used with mean diameters of 0.5 µm and mean lengths of 7 µm. SEM pictures of some selected modifiers are presented in Fig. 12.

The particle sizes of all the used powder fillers are presented in Table 5.

The surface treatment of all inorganic fillers was treated with functional silane (3-(trimethoxysilyl)propyl methacrylate (the Sigma-Aldrich Company). The procedure involved dissolving this liquid in toluene. The aim of the silanization process is to absorb

the active silane groups on the powder surface in a vacuum evaporator. After the silanization process, reactive silane is combined with an inorganic filler and can co-polymerize with the polymer network.

Filler	J-20 glass	PE	PTFE	BN	Si_3N_4
Particle size [mm]	1-3	5	39	5	*Dimension: 0.5 Length: 7*

Table 5. Particle dimensions of fillers

Composites were prepared as shown in Table 6. All the organic constituents were weighed to a porcelain mortar and precisely mixed until uniform polymer paste was obtained. The particles of J-20 glass (57 vol. %) and friction modifiers (3 vol. %) were added to an organic matrix, which had been prepared in advance. Composite A contained an organic matrix and the J-20 filler particles only. The other materials contained also organic or inorganic friction modifiers (3 vol. %) beside containing fluoridated fillers. These organic-inorganic mixtures were then homogenized in a porcelain mortar for 10 minutes. The paste was later placed in cylindrical aluminium moulds (diameter: 3mm; length: 2mm), and it was cured for 40 seconds for each 2-millimetre layer using a Vivadent light-curing system at a wavelength of 420 nm. In order to uncover the analyzed material, the 2-millimetre aluminium envelope was removed. The restored surface was finished by wet grinding with an 800-grit silicon carbide paper. Six specimens were prepared for each composite material.

Material symbol	Component content, [vol. %]		
	Organic matrix	*J-20 glass*	*Friction modifier (3%)*
A	40	60	-
B	40	57	PE
C	40	57	PTFE
D	40	57	Si_3N_4
E	40	57	BN

Table 6. Composition of the materials

The influence of the load and the filler contents on the friction coefficients and wear was estimated. The wear tests were conducted using a pneumatic control pin-on-disk tribotester, which is described in detail elsewhere. The wear machine used in this study was equipped with a spring-sine-cam system allowing cyclic loading of specimens. The samples were the composites presented in Table 6. The samples had average surface areas of $3mm^2$ with the Ra roughness of about 0.1µm. A hardening stainless-steel plate with the hardness of 64 HRC was used as the counterface material due to its relatively high hardness as compared with the hardness of the analyzed materials. The average Ra surface roughness of the counterpart amounted to about 0.1µm. The normal loads were: 1, 5, and 10 MPa. That wear cycle was estimated at the frequency of 1.5 Hz. The wear time was 3 hours, and a sliding wear track of 2.5mm was applied. Prior to the wear tests, the samples and the counterface had been cleaned in distilled water. The wear tests were conducted by means of a special tribotester in the presence of a phosphate buffer (pH of natural saliva - 6.8) as a lubricant. The wear was estimated using the gravimetric method. All the measurements were made after the samples

had been dried in an exsiccator for 24 hours. The mass wear was determined with digital scales to the accuracy of 0.01mg.
The measurements of the friction coefficients using 1 MPa [presented in Fig. 13a] and 10 MPa [presented in Fig. 13b] show that they depend on the kind of filler and loading on the sample.

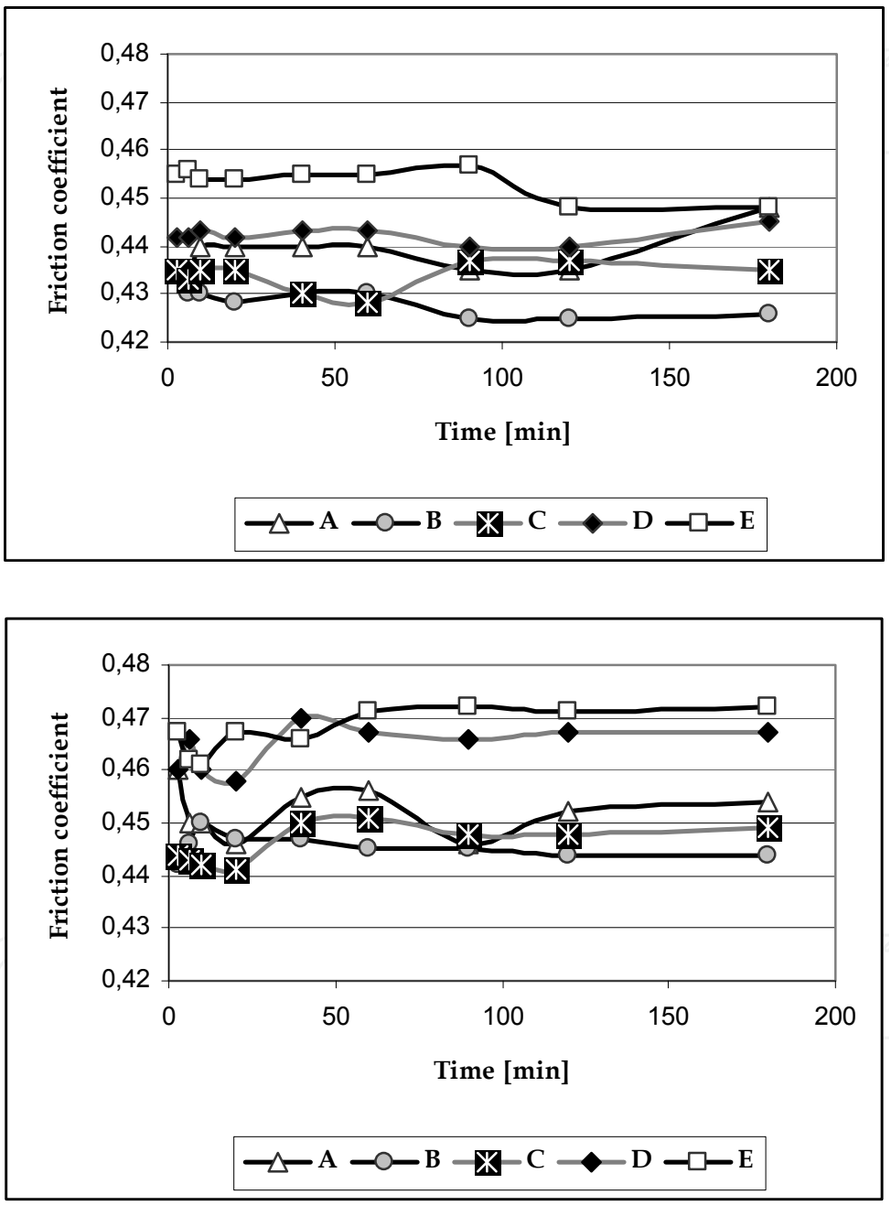

Fig. 13. Influence of time on friction coefficients of investigated materials: a) p=1MPa, b) p=10MPa

The figure illustrates the wear results of the five analyzed composite materials. The first stage of the work consisted in determining the influence of the fluoridated glass filler on the tribological properties. The friction coefficient of this composite material was about 0.45. In

the next stage, the composites with the fluoridated glass filler (J-20) and friction modifiers listed earlier were investigated. At the beginning of the friction processes, the friction coefficient magnitudes ranged from 0.42 to 0.46 for the composites to which the loading of 1 MPa was applied. In the case of the 10 MPa loading, the coefficients ranged from 0.44 to 0.47. This reveals that the friction coefficient increases with the increase of the load. The results show that the friction coefficients are strongly dependent on the kind of the used powder filler. The lowest friction coefficients were observed for the composites with organic friction modifiers (PE and PTFE) , while the biggest friction coefficients were observed for inorganic fillers. The addition of 3 vol.% BN or 3 vol.% Si3N4 increases the composite friction coefficients by about 0.2, while the addition of 3 vol.% PE or PTFE decreases the analyzed parameter. This advantageous effect can be explained by a better adhesion of organic fillers to the organic matrix. The structure of these materials is more enhanced. It is probably a result of these filler grain forms and bonding forces between the fillers and the organic matrix. The improvement of the adhesion of the inorganic glass to the organic resin is achieved through the silanization process. The preparation process applying active silane groups on the powder surface was a process in which active silane groups on the powder surface were drifted. According to some literature sources, such a process does not always improve the mechanical properties of investigated composites. Luo, who analyzed the nanoporous filler structure at inorganic-organic composites, says that application of a silane coupling agent results in a negative effect on the composite wear resistance.

The weight wear of the materials for dental fillings presented in Fig. 14 is the lowest in the case of the composites with organic friction modifiers. The results are correlated with earlier inferences that organic fillers are more firmly connected with the both fluoridated glass filler and the organic polymer matrix. It can be a result of stronger bonding between the polymer basis and organic fillers, due to their original chemical structure. Thus, these particles have some difficulty to spall from the composite material. In addition, the adhesion to the organic matrix was greater. Beside that, the improvement of the wear behaviour of polymeric materials is achieved through applying organic fillers, especially polytetrafluoroethylene, which reduces the adhesion of the material to the counterpart. Inorganic friction modifiers after the silanization process are also obliged to connect with the polymer basis in a chemical way. However, as the results show, such bonding does not suffice and filler particles were chipped during the friction tests. Apparently, there were certain areas in the composites where the bonding of both phases was heterogeneous. These uninterpreted areas are of a brittle nature of unreinforced gel and allow for a greater in-depth crack propagation. The form of the filler particles also influences that process. Therefore, the grinding organic matrix uncovered the filler grains and, as a result of natural abrasive wear, the particles were pulled out from the composite. Additionally, the filler particles in the formulas are significantly harder than the matrix, leading to preferential loss during friction. As it was earlier described, the Si3N4 particles have elongated grain structures, so the materials with the addition of it were the most destructible. Insufficient adhesion of inorganic fillers to organic polymer was probably the other reason for material destruction. The results are different from the inferences of Xu et al., where relatively high wear resistance of the whisker composites were obtained. The results of the wear weight of all the composites suggest that the two-body wear behaviour of these materials depends on the load applied during the test. The wear weight increased by one order of magnitude when

the loading increased from 1 MPa to 10 MPa. The wear of the investigated materials increased with the applied loading.

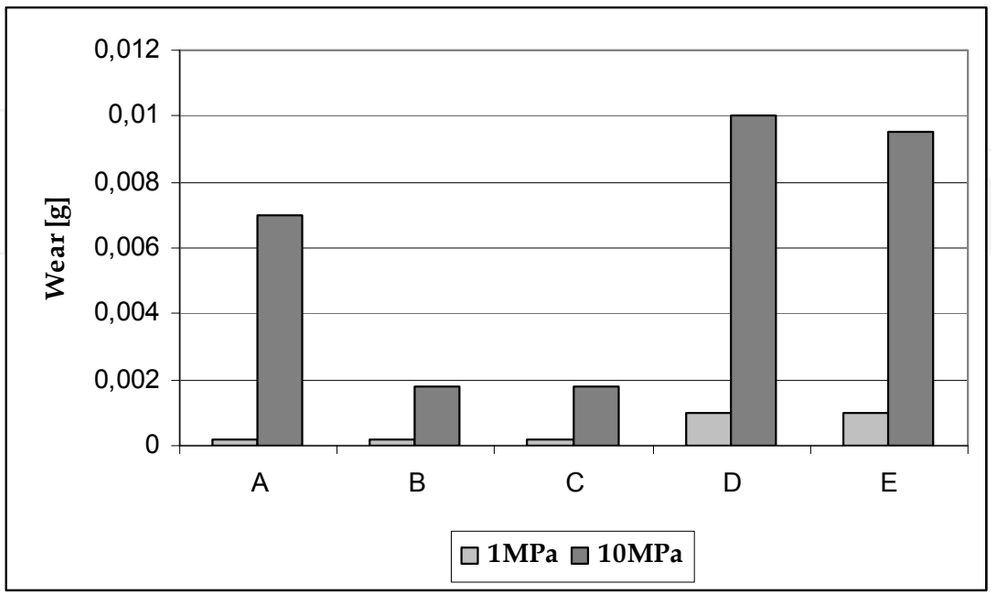

Fig. 14. Wear of investigated materials at loading of 1 and 10MPa

The tribological characteristics of Bis-GMA resin-based composite materials with the addition of fluoridated glass and friction modifiers (PE, PTFE, BN, Si3N4) were investigated. On the basis of the performed examinations, the following conclusions were formulated:

- the wear and friction coefficients of the analyzed materials depend on the filler type and the value of the loading applied to the sample,
- the composites basing on organic fillers as modifiers have the lowest friction coefficients,
- an increase of the loading induces intensification in the wear and friction coefficients.

3.3 Fluoride ions release

At this stage of work, four ceramic-polymer composites containing fluorine sources and nanosilica were tested. All the materials used in this study consisted of 40 vol. % of light-cured organic matrix whose composition was described earlier. The other part of the composite (60 vol. %) was a mixture of inorganic powders: fluorine sources (fluoridated glass J-20, ytterbium fluoride YbF_3) and nanosilica (n-SiO_2). The compound of YbF3 has radiopaque properties additionally. The powders of YbF_3 and nanosilica were delivered from the Sigma-Aldrich Company. Ytterbium fluoride has irregular particles whose mean dimension values were 1μm. The average particle size of nanosilica was 10nm.

The composition of the materials marked with A-D symbols is presented in Table 7. Three specimens were prepared from each composite material for each kind of study. Composite A contains an organic matrix and the J-20 filler powder only. The other materials, beside containing the fluoridated glass, contain also YbF3 or/and nanosilica in the amount of 10 vol. %. All the organic constituents were weighed to a porcelain mortar and precisely mixed until uniform polymer paste was obtained. The J-20 glass particles and other fillers were

added to an organic matrix prepared in advance. These organic-inorganic mixtures were then homogenized in the porcelain mortar for 10 minutes. The paste was then placed on PTFE plates (diameter: 11mm; length: 1mm), and it was cured for 40 seconds using a Vivadent light-curing system at a wavelength of 420 nm. The restored surface was finished by wet grinding with an 800-grit silicon carbide paper.

Materials' symbol	**Component content, [vol. %]**			
	Organic matrix	***J-20 glass***	***YbF3***	***n-SiO_2***
A	40	60	-	-
B	40	50	10	-
C	40	40	10	10
D	40	-	10	-

Table 7. Composition of the materials

For the purpose of determining the content of fluorine released from the examined materials, the method of direct potentiometry with combined fluoride ions selective electrode was used. The prepared materials were placed in 10 ml of a buffer solution of pH of 6.8 in polyethylene containers and the temperature was maintained at 37^0 C. The tests were performed after 1, 4, 7, 14, 30, and 60 days of keeping the samples in the agent solution. TISAB buffer was added to the analyzed solutions before the examination in order to stabilize the pH and eliminate the influence of foreign ions during the examination. Three specimens were prepared of every composite material for each measurement.

The influence of the load and filler content on the fluoride ions release process was estimated. The wear tests were conducted using a pneumatic control pin-on-disk tribotester, which is described in detail elsewhere. The wear machine used in this study was equipped with a spring-sine-cam system allowing cyclic loading of specimens. The samples were the composites presented in Table 7. The samples had average surface areas of 3 mm^2 with the Ra roughness of about 0.1μm. A hardening stainless-steel cylinder with the hardness of 64 HRC was used as the counterface material due to its relatively high hardness as compared with the hardness of the analyzed materials. The average Ra surface roughness of the counterpart amounted to about 0.1μm. The normal loads were: 10, 15, and 20 MPa. That wear cycle was estimated at the frequency of 1.5 Hz. The wear time was 5 hours, and the sliding wear track of 2.5mm was used. Prior to the wear tests, the samples and the counterfaces had been cleaned in distilled water. The friction process was conducted by means of a special tribotester in a phosphate buffer environment with pH=6.8 corresponding to the pH of saliva. Examinations of fluorine release were performed for A, B, C, D materials. The results of the surface roughness research of the specimens were directly measured with a Talysurf 10 profilometry device manufactured by Taylor Hobson. In order to obtain the structure differences before and after fluoride release, studies of the surfaces were performed using a Hitachi S 3000N scanning electron microscope with an attachment for X-ray microanalysis.

The first stage of the work consisted in determining the influence of the various fluoride sources on the amount of fluoride release to the buffer solution. The results of fluoride release from the investigated materials are presented in Fig.15. The results were presented

as the fluoride amount released from 1 mm^2 of the composite material as a function of time. All the tested materials showed accumulative increase in the amount of fluoride in the solutions. It showed, that the highest amounts of the fluoride ions emission were observed for materials A and B.

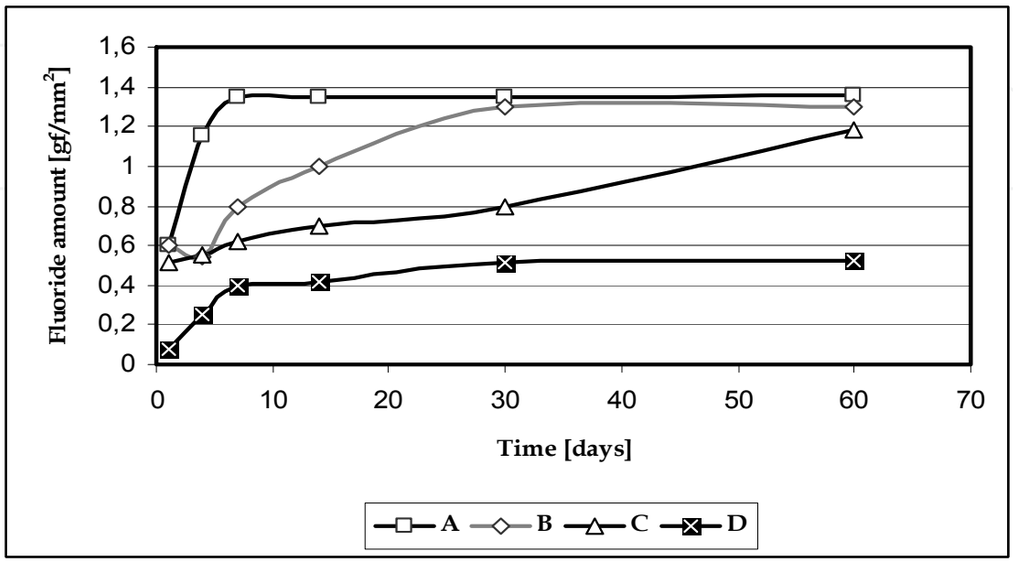

Fig. 15. Amount of fluoride release from tested composites

The maximum peak of fluorine for composite A (about 1.3x10^{-6}g/mm^2) was obtained on the seventh day of the examinations, with a simultaneous stabilization of its level in the solution. It should be noted that the amount of the fluoride release was higher for the composites A and B due to the higher amount of fluoride sources in the materials. At the same time, the fluorine release from the composite with nanosilica (material C) was still growing. For materials C and D, a lower level of fluoride release was observed.

Therefore, the tendency of the emission of fluoride ions from these both composites begins on the 1st day and lasts until the 60th day. In order to estimate the fluoride release after 60 days, a further increase in the exposition time of the composite in the solution is necessary.

The roughness tests of the composite samples after fluoride release reveal some significant differences between the materials. The results presented in Fig. 16 show that the composites with nanoparticles have lower surface roughness (about 0.15 μm) in relation to the composites without that filler.

This can result from the fact of achieving, for this content of nanosilica, a uniform distribution of particles in the composite structure and forming of a more homogenous structure. Consequently, the smaller the filler particles, the lower the surface roughness is. Similar results were obtained in the work of Tagtekin et al. [46]. The estimated parameter is sustained at the limit of 0.11 - 0.19μm for composites A and B, and 0.30μm for composite D. It was also determined that the surface roughness is strongly dependent on the time of the analysis. It could be a result of higher destruction of the material in contact with the buffer solution.

The second stage of the work concerned the estimate of fluoride release from the samples which had earlier undergone the friction process. The main goal of that part of the research

was to determine the influence of cyclic loading on fluoride release from the composites. The measurements of fluoride ion contents in the solutions after the friction tests are presented in Fig. 17.

The results show that the cyclic loadings increase the amount of fluoride ions released. The composites without any loading on them evidently release much lower fluorine levels in contrast to the materials which were tested at different loads. Moreover, the obtained results also show that cyclic loadings intensify fluorine release processes at a later time, when they are immersed in a solution prior to the friction test.

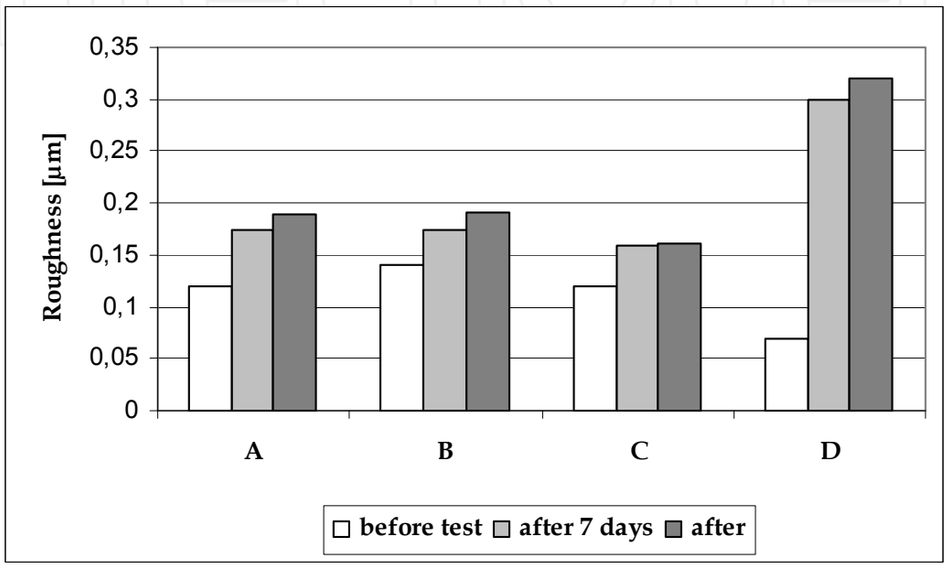

Fig. 16. Surface roughness of tested materials

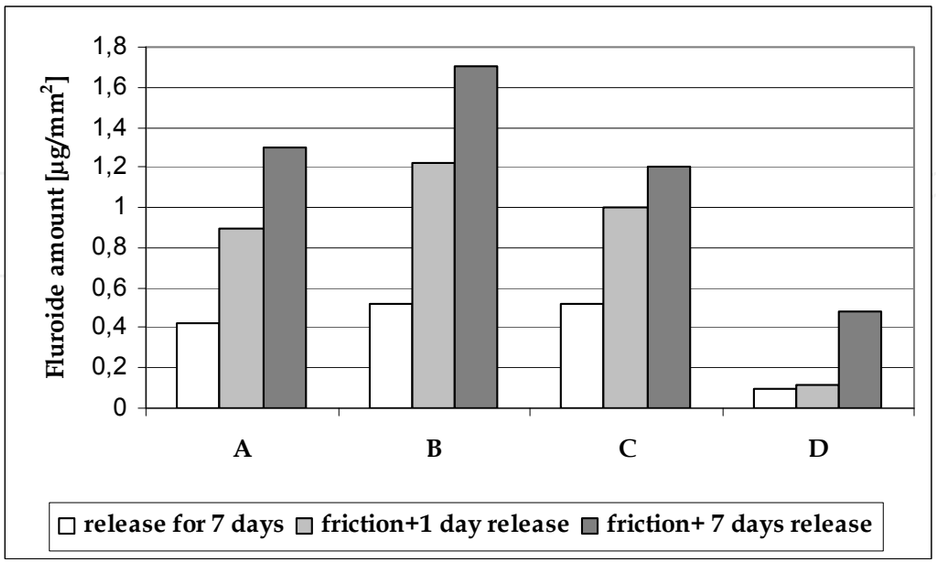

Fig. 17. Influence of cyclic loading and time (p=15MPa) on fluorine release from analyzed composites

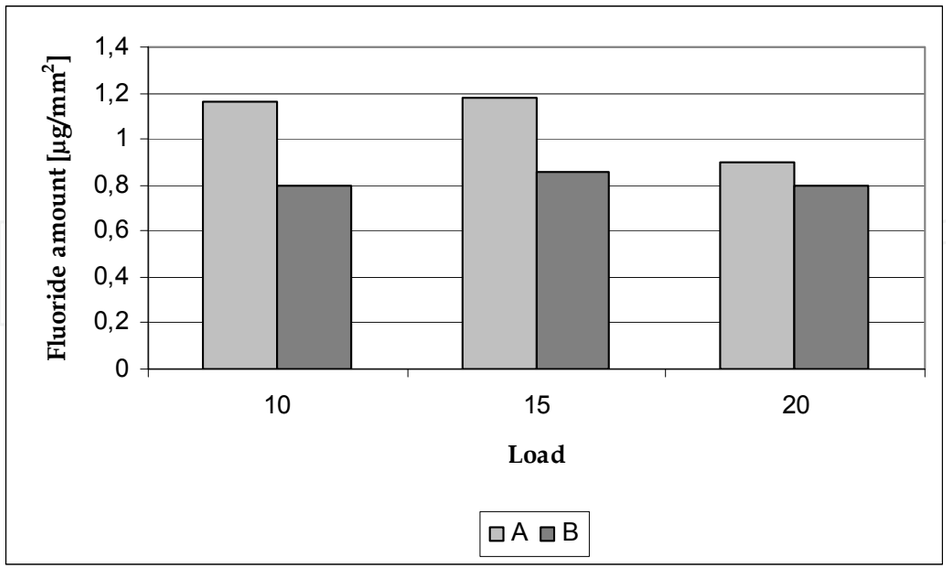

Fig. 18. Influence of loadings (p=10, 15, 20MPa) on fluorine release from analyzed composites

During the 7 days of fluorine emission following the friction process, more concentration was observed in comparison to the 1st day after the friction. It is possible that the wear test changed the internal structure of the materials, and led to the formation of some microcracks. Those discontinuities of the composites can be ways of diffusion for fluoride ions. In consideration of the fact that composites B and C released the highest amount of fluoride ions, they were investigated in successive examinations. The main goal of the planned research was to estimate the influence of the load value on fluoride release. In order to simulate natural forces that occur in the human oral cavity (4-18MPa), three various loads were used: 10, 15, and 20 MPa. The results are presented in Fig. 18.

As the research showed, there is no evident influence of the load value on the amount of fluoride release during the friction process. The amounts of the emitted fluoride ions are comparable in all three value loads. The composite content is more significant. Thus, the presence of nanosilica in a material decreases the fluoride release. It is probably an effect of a low summary content of fluoride sources in composite C in comparison to composite B. Additionally, nanosilica, due to its nanoparticles, could block the diffusion paths for fluoride from the material to the environment solution. Figure 19a shows the surface of composite C with a uniform distribution of the filler particles in this material. The fluoridated glass (symbol J-20) and YbF3 particles before the fluorine release are visible. Figure 19 b shows the structure of composite C after the fluoride ions emission. It proves that numerous microcracks are formed after the friction process.

The observed microcracks may be associated with the interfaces between the filler particles and the resin matrix, which was not enhanced very much. Thus, it can be concluded that during the cyclic loadings, the surface is plastically deformed, and that leads to generating microcracks within the material. These discontinuities, as it was earlier mentioned, are potential paths for diffusing the fluoride ions.

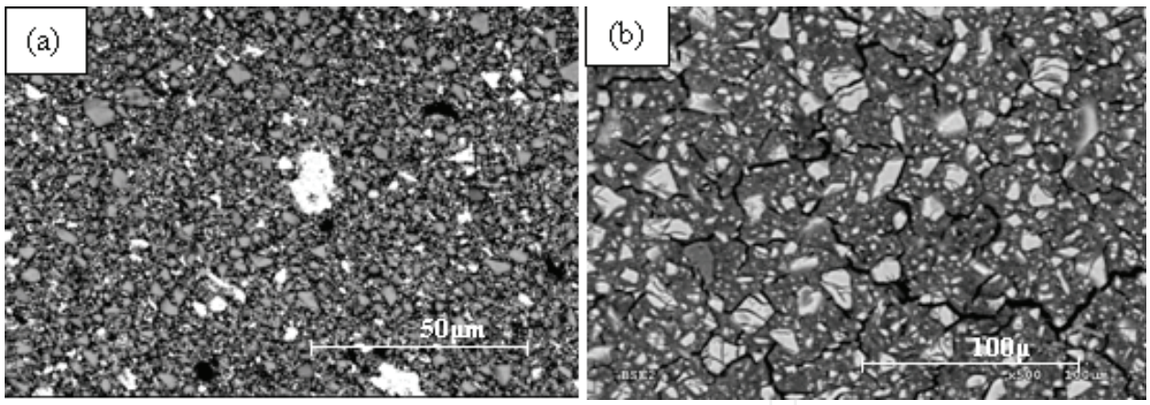

Fig. 19. SEM micrographs of the structure of composite C before (a) and after (b) fluoride release

The influence of the selected fillers and the usage of various loads on releasing the fluoride ions from the analyzed materials were estimated. Taking into account the results of the research, the following conclusions may be formulated:

- the fluoride ions release was observed for all the composite materials,
- the highest level of the fluoride emission occurred in the case of materials based on fluoridated glass,
- nanosilica addition reduces the composite surface roughness during fluoride release as compared to the roughness of the materials without it,
- the fluoride release increases strongly after the cyclic loading process for the analyzed materials, there is no evident relationship between the value of loads applied to the sample and the fluoride release level,

4. References

Dumbleton J.H.: Tribology of natural and artificial Joints. Tribology series 3. Els.Sci.Publ.Co., Amsterdam-Oxford-New York 1983

Dąbrowski J.R.: Tribological aspects of human joints. Tribologia, 1, 1994, 54-63

Grippo J.O., Simring M., Schreiner S.: Attrition, abrasion, corrosion and abfraction revisited. A new perspective on tooth surface lesions. J. Am. Dent. Assoc., 135, 2004, 1109-1118

Cordey J.: Biofunctionality and biomechanics of implant. In: Biomaterials - hard tissue repair and replacement. Els.SciPubl., 1992, 235-245

Dąbrowski J.R., Sajewicz E.: Tribological characteristics of biomaterials. Symp. 'Biomaterials for Medicine and Veterinary Medicine', Kraków (Poland) 1999, pp.245-251

Ungethuem M.: Technologische und biomechanische Aspekte der Hueft-und Kniealloartroplastik. Verlag Haus Huber, Bern-Stuttgart-Wien 1978

Popko J., Dąbrowski J., Dudarew A., Sajewicz A., Iwaszkiewicz B.: Badania tribologiczne stawu biodrowego po założeniu endoprotezy połowiczej w obserwacjach eksperymentalnych. Chir. Narz. Ruchu Ortop. Pol., LXI Supl.3A, 1996, 127-131

Heintze S.D., Zappini G., Rousson V.: Wear of ten dental restorative materials in five wear simulators-results of round robin test. Dent. Mater., 21, 2005, 304-317

Plitz W.: Technologie des kunstlichen Gelenkenersatzes. Expert Verlag, Renninges-Malmsheim 1994

Kramer K.-H.: Implants for surgery – a survey on metallic materials. In: Materials for medical engineering, Band 2, Euromat'99, Viley-VCH Verlag, Munchen 1999, 9-29

Bondarenko W.P.: Tribotiechniczeskije kompozyty z wysokomodulnymi napołnitielami. Izd. Naukowa Dumka, Kijów 1987

Jin Z.M., Dowson D., Fisher J.: Lubrication mechanisms In metal-on-metal hip joint replacements. Proc. 5th World Biomaterials Congress, Toronto 1996, 787

Vancoille E., Celis J.P., Roos J.R.: Tribological and structural characterization of a physical vapour deposited TiC/Ti(C,N)/TiN multilayer. Tribology Int., 26, 1993, 115-119

Mc Kellop H., Park S.-H., Chiesa R., Lu B., Normand P., Doorn P., Amstutz H.: Twenty-year wear analysis of retrieved metal-metal hip prostheses. Proc. 5th World Biomaterials Congress, Toronto 1996, 854

Dorn P.F., Mirra J.M., Campbell P.A., Dorr L.D., van Sambeck K.J.M., Amstutz H.: Pathology of metal on metal total hip prostheses. Proc. 5th World Biomaterials Congress, Toronto 1996,180

Grądzka-Dahlke M., Deptuła P., Dąbrowski J.R.: Properties of composite material based on titanium with graphite addition. 8th World Biomaterials congress, Amsterdam, May 28-June 1, 2008-CD-ROM

S. Klapdohr, N. Moszner: *New Inorganic Components for Dental Filling Composites.* Monatshefte fur Chemie, 136, 2005, pp. 21-45.

J. Luo, R. Seghi, J. Lanutti: *Effect of silane coupling agents on the wear resistance of polymer nanoporous silica gel dental composites.* Mat Sci and Eng, C, 5, 1997, pp. 15-22.

K.S. Wilson, K. Zhang, J.M. Antonucci: *Systematic variation of interfacial phase reactivity in dental nanocomposites.* Biomaterials, 26, 2005, pp. 5095-5103.

X. Xu, J. Burgess: *Compressive strength, fluoride release and recharge of fluoride-releasing materials.* Biomaterials, 24, 2003, pp. 2451-2461.

M. Atai, M. Nekoomanesh, S.A. Hashemi, S. Amani: *Physical and mechanical properties of an experimental dental composite based on a new monomer.* Dental Materials, 20 2004, pp. 663–668.

X.S. Xing, R.K.Y. Li: *Wear behavior of epoxy matrix composites filled with uniform sized submicron silica particles.* Wear, 256, 2004, pp. 21-26.

A.A. Zandinejad, M. Atai, A. Pahlevan: *The effect of ceramic and porous fillers on the mechanical properties of experimental dental composites.* Dental Materials, 22, 2006, pp. 382–387.

K. Friedrich, Z. Zhang, A. Schlarb: *Effects of various fillers on the sliding wear of polymer composites.* Comp Sci and Techn, 65, 2005, pp. 2329-2343.

S. Beun, T. Glorieux, J. Devaux, J. Vreven, G. Leloup: *Characterization of nanofilled compared to universal and microfilled composites.* Dental Materials, 23, 2007, pp. 51–59.

J. Siejka-Kulczyk, J. Mystkowska, M.Lewandowska, J.R.Dabrowski, K.J. Kurzydłowski: *The influence of nano-silica on the wear-resistance of ceramic-polymer composites intended for dental fillings*, Solid State Phenomena, 151, 2009, pp.135-138.

V. Nagarajan, S. Jahanmir, V. Thompson: *In vitro contact wear of dental composites*, Dental Materials, 20, 2004, pp. 63-71.

M. Sulong, R. Aziz: *Wear of materials used in dentistry: A review of the literature*, Journal of Prosthetic Dentistry, 63, 1990, pp. 342-349.

P. Vale Antunes, A. Ramalho: *Study of abrasive resistance of composites for dental restoration by ball-cratering*, Wear, 255, 2003, pp. 990-998.

A.C. Shortall, Q. Hy Xiao, P.M. Marquis: *Potential countersample materials for in vitro simulation wear testing*, Dental Materials, 18, 2002, pp. 246-254.

H.H.K. Xu, J.B. Quinn, A.A. Giuseppetti, F.C. Eichmiller, E.E. Parry, G.E. Schumacher:*Three-body wear of dental resin composites reinforced with silica-fused whiskers*, DentalMaterials, 20, 2004, pp. 220-227.

S.D. Heintze, A. Cavalleri, M. Forjanic, G. Zellweger, V. Rousson: *A comparison of three different methods for the quantification of the in vitro wear of dental materials*, Dental Materials, 22, 2006, pp. 1051-1062.

X. Hu, E. Harrington, P.M Marquis, A.C. Shortall: *The influence of cyclic loading on the wear of a dental composite*, Biomaterials 20, 1999, pp. 907-912.

J. Mystkowska, A. Niewczas, P. Kordos, J.R. Dąbrowski: *Fatigue stress resistance of some composite materials for dental fillings*, Journal of Vibroengineering, 11, 2009, pp. 717-724.

S.D. Heintze, G. Zappini, V. Rousson: *Wear of dental restorative materials in five wear simulators-Results of a round robin test*, Dental Materials, 21, 2005, 304-317.

C.P. Turssi, J.J. Faraoni, M. de Menezes. M.C. Serra: *Analysis of potential lubricants for in vitro wear testing*, Dental Materials, 22, 2006, pp. 77-83.

E.A. Glasspoole, R.L. Erickson, C.L. Davidson: *A fluoride-releasing composite for dental applications,* Dental Materials, 17, 2001, pp. 127-133.

G. Vermeersch, G. Leloup, J. Vreven: *Fluoride release from glass-ionomer cements, compomers and resin composites,* Journal of Oral Rehabilitation, 28, 2001, pp. 26-32.

G. Furtos, V. Cosma, C. Prejmerean, M. Moldovan, M. Brie, A. Colceriu, L. Vensenyi, L. Silaghi-Dumitrescu, C. Sirbu: *Fluoride release from dental resin composites* Mat Sci Eng, 25, 2005, pp. 231-236.

T. Itota, O. Al-Naimi, T.E. Carrick, M. Yoshiyama, J.F. McCabe: *Fluoride release from aged resin composites containing fluoridated glass filler,* Dental Materials, 21, 2005, pp. 1033-1038.

J. Mystkowska, G. Marczuk-Kolada, K. Leszczyńska, J.R. Dąbrowski, J. Karaś: *Fluoride release and antibacterial activity of self-made composite materials for dental fillings*, Solid State Phenomena, 147-149, 2009, pp. 801-806.

J. Mystkowska, G. Rokicki, J. Sidun, J.R. Dąbrowski: *Mechanical and physicochemical properties of some originally made composite materials for dental fillings*, Solid State Phenomena, 165, 2010, pp.142-146.

J. Mystkowska, J.R. Dąbrowski: *The influence of selected powder fillers on tribological properties of composite materials for dental fillings*, Solid State Phenomena, 144, 2009, pp. 33-38.

E. Sajewicz, Z. Kulesza: *A new tribometer for friction and wear studies of dental materials and hard tooth tissues*, Tribology International, 40, 2007, pp. 885-895.

J. Mystkowska: *Fluoride release from composite material for dental fillings*, Solid State Phenomena, 144, 2009, pp. 27-32.

D.A. Tagtekin, F.C. Yarikoglu, F.O. Bozkurt, B. Kologlu, H. Sur: *Selected characteristics of an Ormocer and a conventional hybrid resin composite,* Dental Materials, 20, 2004, pp.487-497.

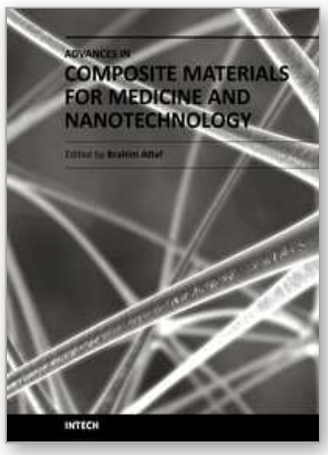

Advances in Composite Materials for Medicine and Nanotechnology

Edited by Dr. Brahim Attaf

ISBN 978-953-307-235-7
Hard cover, 648 pages
Publisher InTech
Published online 01, April, 2011
Published in print edition April, 2011

Due to their good mechanical characteristics in terms of stiffness and strength coupled with mass-saving advantage and other attractive physico-chemical properties, composite materials are successfully used in medicine and nanotechnology fields. To this end, the chapters composing the book have been divided into the following sections: medicine, dental and pharmaceutical applications; nanocomposites for energy efficiency; characterization and fabrication, all of which provide an invaluable overview of this fascinating subject area. The book presents, in addition, some studies carried out in orthopedic and stomatological applications and others aiming to design and produce new devices using the latest advances in nanotechnology. This wide variety of theoretical, numerical and experimental results can help specialists involved in these disciplines to enhance competitiveness and innovation.

INTECH
open science | open minds

InTech Europe
University Campus STeP Ri
Slavka Krautzeka 83/A
51000 Rijeka, Croatia
Phone: +385 (51) 770 447
Fax: +385 (51) 686 166
www.intechopen.com

InTech China
Unit 405, Office Block, Hotel Equatorial Shanghai
No.65, Yan An Road (West), Shanghai, 200040, China
中国上海市延安西路65号上海国际贵都大饭店办公楼405单元
Phone: +86-21-62489820
Fax: +86-21-62489821

IntechOpen